Polymer Chemistry

ROYAL SOCIETY OF CHEMISTRY

PAPER

View Article Online
View Journal | View Issue

Check for updates

Cite this: *Polym. Chem.*, 2025, **16**, 4233

Towards the valorization of poly(acrylic acid) waste: organophotoredox-catalyzed decarboxylative fluorination

Pankti Shabd Mehta, [a,b] Max B. Levy,[a,b] Robert M. O'Dea, [b,c,d] Thomas H. Epps, III *[b,c,d,e] and Mary P. Watson *[a,b,d]

Received 2nd August 2025,
Accepted 4th August 2025

DOI: 10.1039/d5py00774g

rsc.li/polymers

Single-use hygiene products account for a significant volume of landfill waste, and valorization of their superabsorbent polymer component, poly(acrylic acid) (PAA), *via* a polymer-to-polymer transformation has been targeted. Herein, we report the photoredox-catalyzed decarboxylative fluorination of PAA using riboflavin, a sustainable and economical organophotocatalyst. Our approach enables the synthesis of copolymers of PAA and poly(vinyl fluoride) (PVF), valuable commodity materials, in less than one hour of irradiation. Additionally, the process uses water as solvent, applies to PAA substrates of various molecular weights, enables tunable conversion on the basis of irradiation time, and can employ riboflavin from a commercial vitamin B2 capsule as catalyst.

Introduction

Poly(acrylic acid) (PAA) is a highly versatile synthetic polymer known for its exceptional water-absorbing properties.[1–3] Its ability to swell and retain moisture makes PAA a valuable superabsorbent polymer (SAP)[1,4,5] that is employed across various industries, including personal hygiene,[6] agriculture,[7] medicine,[8,9] paint,[10] and detergent.[11] The SAP market was valued at approximately $9.2 billion USD in 2024 and is expected to grow at a compounded annual growth rate of around 5.6% over the next decade.[12] Despite their utility and economic significance, SAPs are prevalent in single-use products and constitute a substantial fraction of plastics waste.[6] Even with recent emphasis on chemical (or advanced) recycling,[6,13–15] a large fraction of these polymers is still either incinerated or disposed of in landfills.[6,16,17]

Valorization *via* polymer-to-polymer transformations has attracted considerable interest from the scientific community as a methodology for plastics waste management.[6,14] A seminal example of this approach was reported by the Li group in 2017, in which they demonstrated the decarboxylative fluorination of PAA with up to 66 mol% vinyl fluoride (VF) repeat units using 18 mol% silver nitrate as a catalyst and SelectFluor as an electrophilic source of fluorine (Scheme 1A).[18] This strategy is an attractive alternative to classic poly(vinyl fluoride) (PVF) synthesis that involves the free radical polymerization of vinyl fluoride, a highly flammable, toxic gas, and often uses forever chemicals (*i.e.*, per- and poly-fluoroalkyl substances (PFAS)) as surfactants.[19,20] Li's method also delivers PAA-*co*-PVF products that would be challenging to create *via* copolymerization of acrylic acid (AA) and VF owing to the vastly different monomer reactivities.[21] These copolymers are interesting because they may be imbued with the advantages of fluorinated polymers (*e.g.*, chemical resistance and durability[19,22,23]) but also have the adhesion properties imparted by carboxylate groups.[24,25] To retain these advantages but avoid the use of 18 mol% of a precious metal catalyst, we conceptualized that photoredox catalysis may provide an attractive and potentially greener alternative, especially if sustainable catalysts could be identified.

Inspired by Sumerlin's work on acridinium-based, photoredox-catalyzed, decarboxylative defunctionalization (and degradation) of polyacrylates (Scheme 1B),[26,27] we prioritized the use of sustainable organophotocatalysts (OPCs) to enable photoredox-catalyzed decarboxylative fluorination of PAA.[28–31] In addition to having tunable electronic properties, OPCs are appealing as they avoid the use of rare metals and are considered environmentally benign, thereby aligning with the goals of both use of renewable feedstocks and catalysis in green chemistry.[31–35] However, OPC-catalyzed decarboxylative

[a]*Department of Chemistry and Biochemistry, University of Delaware, Newark, Delaware 19716, USA. E-mail: mpwatson@udel.edu*
[b]*Center for Plastics Innovation, University of Delaware, Newark, Delaware 19716, USA*
[c]*Department of Chemical and Biomolecular Engineering, University of Delaware, Newark, Delaware 19716, USA. E-mail: thepps@udel.edu*
[d]*Center for Research in Soft matter and Polymers (CRiSP), University of Delaware, Newark, Delaware 19716, USA*
[e]*Department of Materials Science and Engineering, University of Delaware, Newark, Delaware 19716, USA*

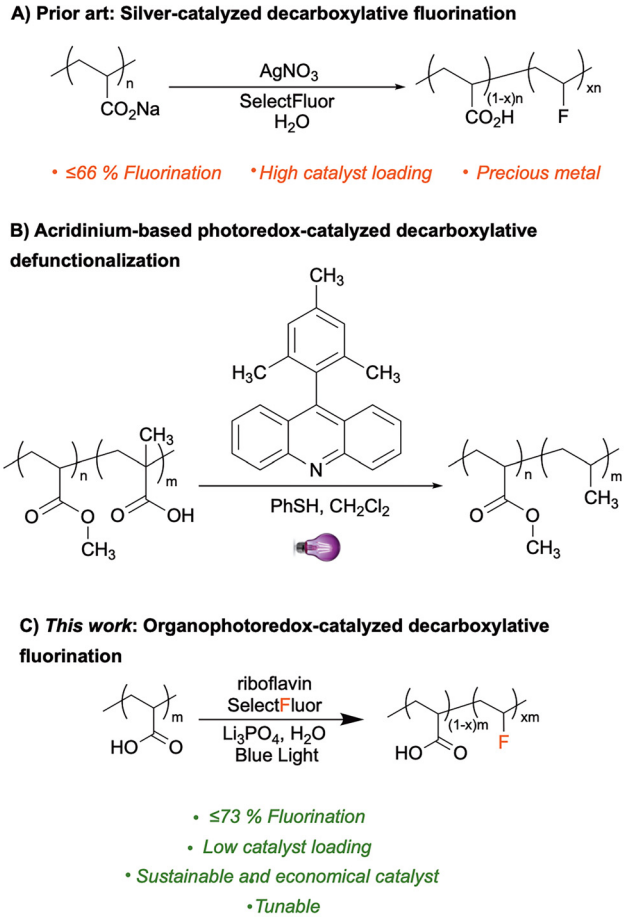

Scheme 1 Decarboxylative functionalization of polyacrylates (A) silver-catalyzed decarboxylative fluorination; (B) acridinium-based, photoredox-catalyzed, decarboxylative defunctionalization; (C) this work: organophotoredox-catalyzed decarboxylative fluorination. *x* = mole fraction VF (applies to all figures).

fluorinations of small molecules have predominantly employed acridinium-based photocatalysts that are expensive and have limited commercial availability and solubility.[30,36,37] To address these limitations, we prioritized the use of riboflavin (vitamin B2) as a more cost-effective and environmentally friendly alternative.[38] Herein, we demonstrate a simple approach to generating fluorinated polymers from PAA using riboflavin, highlighting riboflavin's potential for environmentally benign polymer functionalization and establishing important proof-of-concept for the feasibility of decarboxylative functionalizations of waste polymers (Scheme 1C).

Results and discussion

Synthesis of PAA with an internal fluorine standard

The ability to rapidly assess the impact of various reaction parameters on the efficiency of the decarboxylative fluorination was crucial for the successful development of this approach. Thus, we sought an analytical method that would allow us to quantitatively analyse crude reaction mixtures. ^{1}H nuclear magnetic resonance (NMR) spectroscopy was an initial choice; however, the broadness of the ^{1}H NMR spectroscopy peaks of PAA and its fluorinated derivatives hampered the accuracy of quantification by this method. Recognizing that ^{19}F NMR spectroscopy would provide sharper signals with better resolution between peaks, we prepared a model PAA substrate functionalized with a trifluorotolyl end group. This model PAA was synthesized using fluorine-labelled RAFT (Reversible Addition–Fragmentation Chain Transfer) agent **3** that was prepared *via* amide coupling (Scheme 2). RAFT polymerization of acrylic acid with RAFT agent **3** yielded PAA **4**. The trithiocarbonyl end group was then cleaved using 2,2′-azobis(isobutyronitrile) (AIBN) and lauroyl peroxide (LPO) to avoid potential side reactions of this group under the radical conditions needed for photoredox-catalyzed decarboxylative fluorination. Fluorine-labelled PAA **5** was then used for all optimization studies. The fluorinated end group of PAA **5** has distinct signals in both the aliphatic and aromatic regions of the ^{1}H and ^{19}F NMR spectra, enabling rapid and direct quantification of the extent of decarboxylative fluorination by comparison of these peaks to those of the VF repeat unit. As detailed in the SI, these values were internally consistent and agreed with quantification of VF incorporation *via* comparison of the ratio of ^{1}H NMR spectroscopy peaks of the VF and AA repeat units, along with elemental analysis of the purified polymer products.

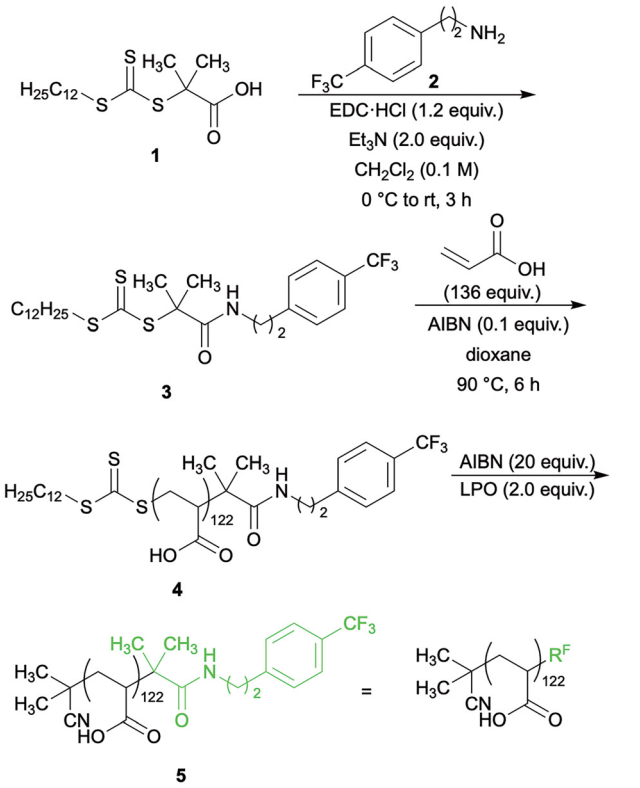

Scheme 2 Synthesis of PAA with fluorinated end group. EDC·HCl = 1-ethyl-3-(3-dimethylaminopropyl)carbodiimide hydrochloride salt.

Organophotocatalyst identification

Our optimization studies began by evaluating a series of organophotocatalysts in the decarboxylative fluorination of model PAA **5**. Acridinium photocatalysts OPC **1–3** and cyanobenzene OPC **4** are well precedented in decarboxylative reactions of small molecule substrates.[29,30] These catalysts provided 45–67 mol% VF incorporation under our initial conditions (Table 1, entries 1–4). Analogous to studies with small molecule carboxylic acids, eosin Y (OPC **5**) and rose bengal (OPC **6**) gave lower conversions (entries 5 and 6).[30] Riboflavin (OPC 7) also has been investigated in small molecule decarboxylations,[29,30] but typically it is less efficient than OPCs **1–4**. However, in the decarboxylative fluorination of our polymer substrate, riboflavin exhibited comparable performance to these more expensive organophotocatalysts (entry 7). To improve the potential for economic and environmental sustainability, we pursued further optimization using riboflavin as the photocatalyst.

Table 1 OPC screen[a]

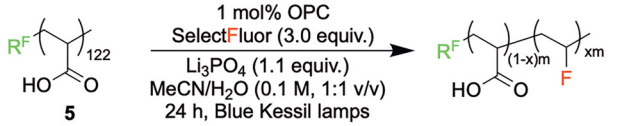

Entry	OPC	Mol% VF[b]
1	OPC **1**	67[c]
2	OPC **2**	45
3	OPC **3**	65
4	OPC **4**	64[c]
5	OPC **5**	30
6	OPC **6**	26
7	OPC 7 (riboflavin)	63

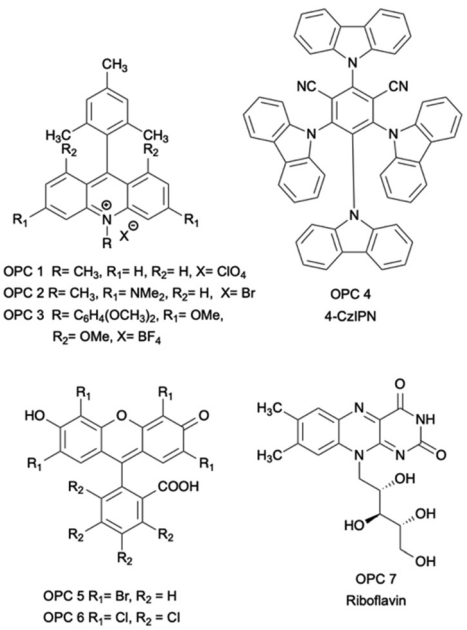

[a] Conditions: PAA (1.0 mmol, 72 mg), OPC (1 mol%), Li_3PO_4 (1.1 mmol, 127 mg), SelectFluor (3.0 mmol, 1.06 g), MeCN : H_2O (0.1 M, 1 : 1 v/v, 10 mL). [b] mol% VF = (x × 100). Determined by ^{19}F NMR spectroscopy analysis of VF repeat units compared to the CF_3 end group. See SI for additional details and mol% VF by ^{1}H NMR spectroscopy. [c] Because poor solubility of copolymer product in dimethylsulfoxide (DMSO) gave poor signal-to-noise by ^{19}F NMR spectroscopy, mol% VF was calculated using ^{1}H NMR spectroscopy.

Optimization

Having established the catalytic efficiency of riboflavin, the impacts of the other reaction parameters were assessed. Although acetonitrile (MeCN)/H_2O mixtures are often used for small molecule decarboxylations to ensure the solubility of organophotocatalysts and small molecule substrates,[30] riboflavin, PAA, and SelectFluor are all water soluble, suggesting that MeCN may be unnecessary. Indeed, the use of water as the sole solvent gave similar conversion as the MeCN/H_2O conditions, simplified reaction setup, and improved process sustainability (Table 2, entries 1 and 2).

Decreasing the amount of catalyst to 0.1 mol% led to a significant drop in the extent of fluorination while increasing the amount of catalyst did not yield a higher conversion above 1 mol% (entries 2–5). SelectFluor was uniquely reactive; other electrophilic sources of fluorine such as *N*-fluorobenzenesulfonamide and *N*-fluoropyridinium triflate led to no fluorination (entries 6 and 7). On the other hand, increasing the amount of SelectFluor to more than two equivalents did not benefit the reaction (entries 8–10). Finally, different inorganic bases did not impact the extent of fluorination (Table S3).

Although pleased to observe similar VF incorporation as Li's $AgNO_3$-catalyzed conditions, we sought to understand why conversion was capped at 68 mol% VF incorporation in our model substrate (Table 2, entry 9). One possibility was catalyst death or unproductive consumption of SelectFluor; however, higher fluorination was not observed by adding an additional

Table 2 Optimization studies

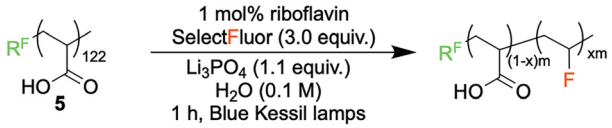

Entry	Deviation from standard conditions[a]	Mol% VF[b]
1	MeCN/H_2O (0.1 M, 1 : 1 v/v)	63
2	—	65
3	0.1 mol% riboflavin	39
4	2.5 mol% riboflavin	64
5	5.0 mol% riboflavin	62
6	*N*-Fluorobenzenesulfonamide	n.d.[c]
7	*N*-Fluoropyridinium triflate	n.d.[c]
8	1.1 equiv. SelectFluor	57
9	2.0 equiv. SelectFluor	68
10	4.0 equiv. SelectFluor	60

[a] Standard conditions: PAA (1.0 mmol, 72 mg), riboflavin (1 mol%), Li_3PO_4 (1.1 mmol, 127 mg), SelectFluor (3.0 mmol, 1.06 g), H_2O (0.1 M, 1 : 1 v/v, 10 mL). [b] mol% VF = (x × 100). Determined by ^{19}F NMR spectroscopy analysis of VF repeat units compared to the CF_3 end group. See SI for additional details and mol% VF by ^{1}H NMR spectroscopy analysis. [c] Not detected.

1 mol% riboflavin or an additional two equivalents of SelectFluor after 1 h of reaction time (Table 3, entries 1 and 2), suggesting that neither catalyst death nor SelectFluor decomposition were the issue. To investigate if the high intensity light from the Kessil lamps was detrimental, we used blue LEDs, but similar conversion was reached (entry 3). These experiments, along with Li's results, suggest that the solubility of the PAA-*co*-PVF product may be the limiting factor in capping conversion at 68 mol%. Estimated solubility parameters from group contribution theory further support this hypothesis as the total solubility parameter (δ_{total}) drops substantially as fluorination increases – the value decreased by 5.2 $MPa^{1/2}$ from pure PAA (δ_{total} = 21.6 $MPa^{1/2}$) to 68 mol% PVF (δ_{total} = 16.3 $MPa^{1/2}$).[39,40]

Control reactions confirmed that light and catalyst are required (Table 3, entries 4 and 5). Without base, 11 mol% VF was achieved, consistent with observations in small molecule decarboxylations (entry 6).[41] Excitingly, nutrition-grade riboflavin from a commercial vitamin B2 capsule can also be used as catalyst, giving 62 mol% VF (entry 7).

Tunability of fluorination with duration of irradiation

In addition to using natural riboflavin as catalyst and water as solvent, an advantage of this photoredox-catalyzed approach is the ability to tune the extent of fluorination by the length of light exposure. Even using milder (and less expensive) blue LEDs, this reaction was remarkably fast. Conversion to 33 mol% VF was achieved within 5 min of irradiation (Table 4, entry 1), increasing to 63 mol% in 60 min, after which conversion plateaued.[42] This method thus allows for tuneable fluorination by altering the extent of irradiation.

Table 3 Control experiments

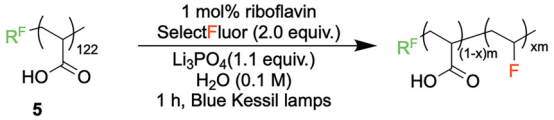

Entry	Deviation from standard conditions[a]	Mol% VF[b]
1	Additional 1 mol% catalyst	58
2	Additional 2.0 equiv. SelectFluor	63
3	Blue LEDs	63
4	No light	<5
5	No catalyst	<5
6	No base	11
7	Vit. B2 capsule[c]	62

[a] Standard conditions: PAA (1.0 mmol, 72 mg), riboflavin (1 mol%, 3.8 mg), Li_3PO_4 (1.1 mmol, 127 mg), SelectFluor (2.0 mmol, 704 mg), H_2O (0.1 M, 10 mL). [b] mol% VF = (x × 100). Determined by ^{19}F NMR spectroscopy analysis of VF repeat units compared to the CF_3 end group. See SI for additional details and mol% VF by ^1H NMR spectroscopy analysis. [c] A commercial vitamin B2 capsule was opened, and the powder contents were weighed (194 mg). According to the nutrition label, the capsule contained 100 mg of riboflavin, which accounted for 52% of the total powder mass. Accordingly, 7.4 mg of the capsule powder (equivalent to approximately 3.8 mg and 0.010 mmol of riboflavin) was added to the reaction mixture as the catalyst.

Table 4 Effect of duration of irradiation on mol% fluorination[a]

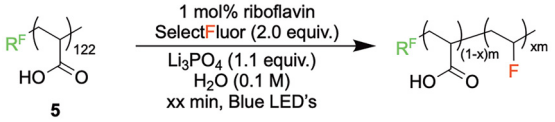

Entry	Duration of irradiation (min)	Mol% VF[b]	Yield[c] (%)
1	5	33	73
2	15	48	65
3	30	56	61
4	45	62	64
5	60	63	67
6	360	63	67
7	1440	66	60

[a] Standard conditions: PAA (2.0 mmol, 144 mg), riboflavin (1 mol%, 7.6 mg), Li_3PO_4 (1.1 mmol, 254 mg), SelectFluor (2.0 mmol, 1.42 g), H_2O (0.1 M, 20 mL). [b] mol% VF = (x × 100). Determined by ^{19}F NMR spectroscopy of VF repeat units compared to the CF_3 end group. See SI for additional details and mol% VF by ^1H NMR spectroscopy and elemental analysis. [c] % Yield = [a/(mmol AA repeat units × (72 − 26x))] (100%), a = mg of isolated copolymer, x = mole fraction VF.

Investigation of chain coupling

Methylation of the polymer products from our time screen provided soluble poly[(methyl acrylate)-*co*-VF] polymers for gel permeation chromatography (GPC) analysis (see SI for details). The GPC traces displayed bimodality that was not present in the chromatogram of the methyl ester of PAA **5**. This bimodality is consistent with formation of a copolymer of higher molecular weight (retention time ~18.5 min) in addition to the major copolymer product (retention time ~20 min, Fig. 1A). Peaks appearing at ~22 min are attributable to residual water and/or acetone in the polymer after dialysis and lyophilization and are unrelated to the polymer itself. The appearance of the higher molecular weight polymer shoulder was particularly apparent when increasing the duration of irradiation above 45 min. We hypothesize that rapid radical formation, and thus high radical concentration, leads to chain coupling/crosslinking as polymer backbone radicals terminate with one another. By fitting these GPC peaks to two Gaussian curves (Fig. S4), the percent coupled fraction was estimated to be 4–22% (Table S7), plateauing at ~60 min irradiation time (Fig. 1C, blue dots). This plateauing suggests that the polymer chains adopt a tighter conformation in solution and, eventually, precipitate out as the degree of fluorination (*i.e.*, irradiation time) increases. Furthermore, the polymer yield similarly plateaued (Table S7, Fig. S5), indicating that further coupling to form larger polymers or crosslinked networks was minimal.

We hypothesized that a relatively low concentration of backbone radical to SelectFluor would minimize crosslinking. Indeed, increasing the concentration of SelectFluor to promote fluorination over crosslinking reactions resulted in a nearly unimodal GPC chromatogram (Fig. 1B). Fitting this GPC peak to two Gaussian curves estimated that the percent coupled fraction was 13% (Fig. 1C). Reducing the intensity of light is

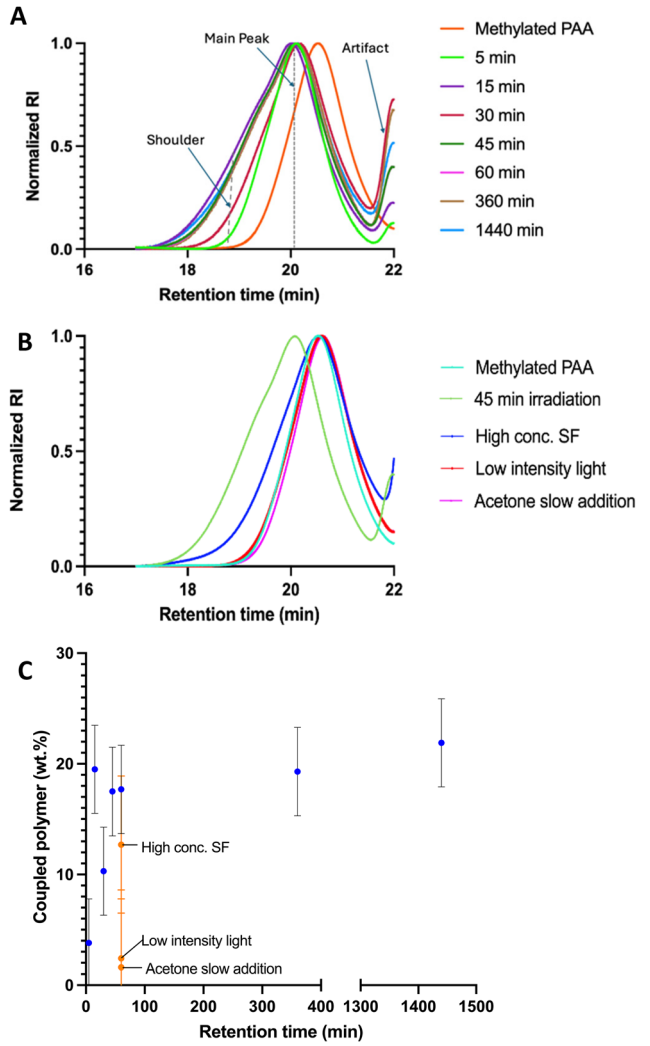

Fig. 1 GPC traces of methylated polymer products for (A) effect of duration of irradiation (Note: the 60 min trace overlaps with the traces for 45 and 360 min), (B) investigation of chain coupling upon changes to concentration and irradiation, (C) fraction of coupled polymer *vs.* irradiation time under Table 4 conditions (blue dots) and upon changes to concentration and irradiation (orange dots). Error bars show approximate error based on the standard deviation of wt. % of coupled polymer for irradiation times ≥15 min.

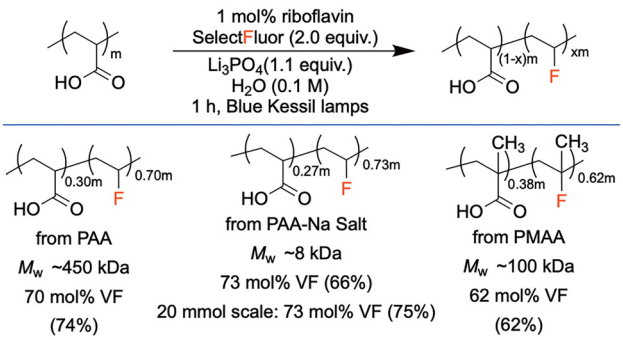

Scheme 3 Riboflavin photoredox-catalyzed decarboxylative fluorination of commercial poly(meth)acrylates. Mol% VF determined by elemental analysis and equal to (x × 100). Yield % indicated in brackets, calculated using the formula [a/(mmol AA repeat units × (72 − 26x))] (100%), a = mg of isolated copolymer, x = mole fraction VF for PAA-derived copolymers, and [a/(mmol MAA repeat units × (86 − 26x))] (100%) for PMAA copolymer.

another handle to lower the rate of radical generation and thus the radical concentration. Similar to the experiment with increased SelectFluor loading, the GPC chromatogram of the copolymer formed with less intense light was again unimodal, indicating minimal, if any, crosslinking occurred (2% by Gaussian fitting, Fig. 1C). We also hypothesized that solubility likely plays a role in the crosslinking reaction. To this end, acetone (degassed with N_2), which dissolves the copolymer, was slowly fed into the reaction mixture over the course of the reaction to prevent the copolymer chains from adopting a tighter conformation. The resulting copolymer exhibited a lower degree of fluorination relative to the experiment without acetone (54% *vs.* 66%), but the GPC chromatogram was again almost unimodal (2% by Gaussian fitting, Fig. 1C), indicating that both radical concentration and solubility play important roles in the cross-linking of polymer chains under photoredox-catalyzed decarboxylative fluorination conditions.

Application to commercial samples

To evaluate the generality of the transformation, we tested a range of commercially available substrates, as illustrated in Scheme 3.[42] The fluorination was effective on high molecular weight PAA (M_W ~ 450 kDa) and resulted in 70 mol% VF incorporation. Using acidified sodium polyacrylate (M_W ~ 8 kDa), 73 mol% VF incorporation was reached on a 2 mmol scale. The same level of VF incorporation was also observed on a 20 mmol scale. Finally, poly(methacrylic acid) (PMAA) (M_W ~ 100 kDa) was also an effective substrate, delivering a P(MAA-*co*-propylene fluoride) copolymer with 62 mol% conversion.

Conclusions

In summary, we report that riboflavin is an effective catalyst for the photoredox-catalyzed decarboxylative fluorination of PAA and PMAA. This method offers an efficient method to convert common SAPs to fluorinated copolymer products with conversions up to 73 mol% fluorinated repeat units. Additional advantages include utility across a broad range of molecular weights and the opportunity to use water as a green solvent. Furthermore, nutrition-grade riboflavin from a commercial vitamin B2 capsule can also be used as catalyst, demonstrating that reagent-grade riboflavin is not required. This work also highlights ongoing challenges in decarboxylative polymer functionalizations *via* radical intermediates; careful control of radical concentration and polymer solubility are critical to bring these methods into industrial use. Solving these challenges and applying riboflavin catalysts to other polymer functionalizations provides a fertile ground for future reaction development.

Author contributions

P. S. M., R. M. O., T. H. E., and M. P. W. conceived and designed the experiments. M. B. L. designed and prepared model polymer **5**. P. S. M. conducted all other synthetic experiments. P. S. M. and R. M. O. conducted characterization and analysis of all polymer products. All authors helped analyse the data and contributed to the writing of this manuscript.

Conflicts of interest

There are no conflicts to declare.

Data availability

The data supporting this article have been included as part of the SI.

Full experimental details, characterization data including ^{1}H, ^{13}C, and ^{19}F NMR spectra, elemental analysis, DSC thermograms, TGA plots, and supplemental experiments. See DOI: **https://doi.org/10.1039/d5py00774g**.

Acknowledgements

This work was supported as part of the Center for Plastics Innovation, an Energy Frontier Research Center funded by the U.S. Department of Energy, Office of Science, Basic Energy Sciences at the University of Delaware under award # DE-SC0021166.

References

1 J. E. Elliott, M. Macdonald, J. Nie and C. N. Bowman, Structure and swelling of poly(acrylic acid) hydrogels: effect of pH, ionic strength, and dilution on the crosslinked polymer structure, *Polymer*, 2004, **45**(5), 1503–1510, DOI: **10.1016/j.polymer.2003.12.040**.

2 J. R. Witono, I. W. Noordergraaf, H. J. Heeres and L. P. B. M. Janssen, Water absorption, retention and the swelling characteristics of cassava starch grafted with polyacrylic acid, *Carbohydr. Polym.*, 2014, **103**, 325–332, DOI: **10.1016/j.carbpol.2013.12.056**.

3 M. Zhang, Z. Cheng, T. Zhao, M. Liu, M. Hu and J. Li, Synthesis, Characterization, and Swelling Behaviors of Salt-Sensitive Maize Bran–Poly(acrylic acid) Superabsorbent Hydrogel, *J. Agric. Food Chem.*, 2014, **62**(35), 8867–8874, DOI: **10.1021/jf5021279**.

4 J. Zhang, Q. Wang and A. Wang, Synthesis and characterization of chitosan-g-poly(acrylic acid)/attapulgite superabsorbent composites, *Carbohydr. Polym.*, 2007, **68**(2), 367–374, DOI: **10.1016/j.carbpol.2006.11.018**.

5 Z. S. Liu and G. L. Rempel, Preparation of superabsorbent polymers by crosslinking acrylic acid and acrylamide copolymers, *J. Appl. Polym. Sci.*, 1997, **64**(7), 1345–1353, DOI: **10.1002/(SICI)1097-4628(19970516)64:7<1345::AID-APP14>3.0.CO;2-W**.

6 P. T. Chazovachii, M. J. Somers, M. T. Robo, D. I. Collias, M. I. James, E. N. G. Marsh, P. M. Zimmerman, J. F. Alfaro and A. J. McNeil, Giving superabsorbent polymers a second life as pressure-sensitive adhesives, *Nat. Commun.*, 2021, **12**(1), 4524, DOI: **10.1038/s41467-021-24488-9**.

7 L. Chang, L. Xu, Y. Liu and D. Qiu, Superabsorbent polymers used for agricultural water retention, *Polym. Test.*, 2021, **94**, 107021, DOI: **10.1016/j.polymertesting.2020.107021**.

8 W. Chen, S. Zhou, L. Ge, W. Wu and X. Jiang, Translatable High Drug Loading Drug Delivery Systems Based on Biocompatible Polymer Nanocarriers, *Biomacromolecules*, 2018, **19**(6), 1732–1745, DOI: **10.1021/acs.biomac.8b00218**.

9 T. N. Pashirova, A. B. Afonso, N. V. Terekhova, M. I. Kamalov, P. Masson and E. B. Souto, Chapter 5 - Nanogels for drug delivery: physicochemical properties, biological behavior, and in vivo applications, in *Nanotechnology and Regenerative Medicine*, ed. M. H. Santana, E. B. Souto and R. Shegokar, Academic Press, 2023, pp. 95–131.

10 J. M. Friel, E. Nungesser and J.V. Koleske, Acrylic Polymers as Coatings Binders, in *Paint and Coating Testing Manual: 15th. Edition of the Gardner-Sward Handbook*, 2012, Vol. MNL17-2ND-EB, pp. 49–64.

11 M. K. Nagarajan, Multi-functional polyacrylate polymers in detergents, *J. Am. Oil Chem. Soc.*, 1985, **62**(5), 949–955, DOI: **10.1007/BF02541766**.

12 Super Absorbent Polymer Market Growth – Trends & Forecast 2024–2034; **https://www.futuremarketinsights.com/reports/super-absorbent-polymer-market**.

13 H. S. Wang, M. Agrachev, H. Kim, N. P. Truong, T.-L. Choi, G. Jeschke and A. Anastasaki, Visible light–triggered depolymerization of commercial polymethacrylates, *Science*, 2025, **387**(6736), 874–880, DOI: **10.1126/science.adr1637**.

14 A. B. Korpusik, A. Adili, K. Bhatt, J. E. Anatot, D. Seidel and B. S. Sumerlin, Degradation of Polyacrylates by One-Pot Sequential Dehydrodecarboxylation and Ozonolysis, *J. Am. Chem. Soc.*, 2023, **145**(19), 10480–10485, DOI: **10.1021/jacs.3c02497**.

15 L. T. J. Korley, T. H. Epps, III, B. A. Helms and A. J. Ryan, Toward polymer upcycling—adding value and tackling circularity, *Science*, 2021, **373**(6550), 66–69, DOI: **10.1126/science.abg4503**.

16 A. S. Gadtya, D. Tripathy and S. Moharana, Recycling and Reuse of Superabsorbent Polymers, in *Bio-based Superabsorbents: Recent Trends, Types, Applications and Recycling*, ed. S. Pradhan and S. Mohanty, Springer Nature Singapore, 2023, pp. 161–183.

17 J. Chen, J. Wu, P. Raffa, F. Picchioni and C. E. Koning, Superabsorbent Polymers: From long-established, microplastics generating systems, to sustainable, biodegradable

and future proof alternatives, *Prog. Polym. Sci.*, 2022, **125**, 101475, DOI: 10.1016/j.progpolymsci.2021.101475.

18 Y. Dong, Z. Wang and C. Li, Controlled radical fluorination of poly(meth)acrylic acids in aqueous solution, *Nat. Commun.*, 2017, **8**(1), 277, DOI: 10.1038/s41467-017-00376-z.

19 M. H. Alaaeddin, S. M. Sapuan, M. Y. M. Zuhri, E. S. Zainudin and F. M. Al-Oqla, Polyvinyl fluoride (PVF); Its Properties, Applications, and Manufacturing Prospects, *IOP Conf. Ser. Mater. Sci. Eng.*, 2019, **538**(1), 012010, DOI: 10.1088/1757-899X/538/1/012010.

20 J. Gardiner, Fluoropolymers: Origin, Production, and Industrial and Commercial Applications, *Aust. J. Chem.*, 2015, **68**(1), 13–22, DOI: 10.1071/CH14165.

21 U. U. Kh, T. S. Sirlibaev and A. A. Yul'chibaev, Vinyl Fluoride Polymers, *Russ. Chem. Rev.*, 1977, **46**(5), 462, DOI: 10.1070/RC1977v046n05ABEH002147.

22 L. McKeen and S. Ebnesajjad, Chapter 22 - Chemical resistance of polyvinyl fluoride and polyvinylidene fluoride, in *Handbook of Thermoplastic Fluoropolymers*, ed. L. McKeen and S. Ebnesajjad, William Andrew Publishing, 2023, pp. 403–414.

23 6 - Introduction to Fluoropolymers, in *Introduction to Fluoropolymers*, ed. Ebnesajjad, S., William Andrew Publishing, 2013, pp 63–89.

24 J. Sakdapipanich, N. Thananusont and N. Pukkate, Synthesis of acrylate polymers by a novel emulsion polymerization for adhesive applications, *J. Appl. Polym. Sci.*, 2006, **100**(1), 413–421, DOI: 10.1002/app.23117.

25 H. T. Lam, O. Zupančič, F. Laffleur and A. Bernkop-Schnürch, Mucoadhesive properties of polyacrylates: Structure – Function relationship, *Int. J. Adhes. Adhes.*, 2021, **107**, 102857, DOI: 10.1016/j.ijadhadh.2021.102857.

26 J. B. Garrison, R. W. Hughes, J. B. Young and B. S. Sumerlin, Photoinduced SET to access olefin-acrylate copolymers, *Polym. Chem.*, 2022, **13**(7), 982–988, DOI: 10.1039/D1PY01643A.

27 A. Adili, A. B. Korpusik, D. Seidel and B. S. Sumerlin, Photocatalytic Direct Decarboxylation of Carboxylic Acids to Derivatize or Degrade Polymers, *Angew. Chem., Int. Ed.*, 2022, **61**(40), e202209085, DOI: 10.1002/anie.202209085.

28 N. P. Ramirez and J. C. Gonzalez-Gomez, Decarboxylative Giese-Type Reaction of Carboxylic Acids Promoted by Visible Light: A Sustainable and Photoredox-Neutral Protocol, *Eur. J. Org. Chem.*, 2017, (15), 2154–2163, DOI: 10.1002/ejoc.201601478.

29 C. Fischer, C. Kerzig, B. Zilate, O. S. Wenger and C. Sparr, Modulation of Acridinium Organophotoredox Catalysts Guided by Photophysical Studies, *ACS Catal.*, 2020, **10**(1), 210–215, DOI: 10.1021/acscatal.9b03606.

30 X. Wu, C. Meng, X. Yuan, X. Jia, X. Qian and J. Ye, Transition-metal-free visible-light photoredox catalysis at room-temperature for decarboxylative fluorination of aliphatic carboxylic acids by organic dyes, *Chem. Commun.*, 2015, **51**(59), 11864–11867, DOI: 10.1039/C5CC04527D.

31 A. Joshi-Pangu, F. Lévesque, H. G. Roth, S. F. Oliver, L.-C. Campeau, D. Nicewicz and D. A. DiRocco, Acridinium-Based Photocatalysts: A Sustainable Option in Photoredox Catalysis, *J. Org. Chem.*, 2016, **81**(16), 7244–7249, DOI: 10.1021/acs.joc.6b01240.

32 M. V. Bobo, J. J. Kuchta and A. K. Vannucci, Recent advancements in the development of molecular organic photocatalysts, *Org. Biomol. Chem.*, 2021, **19**(22), 4816–4834, DOI: 10.1039/D1OB00396H.

33 S. Fukuzumi, H. Kotani, K. Ohkubo, S. Ogo, N. V. Tkachenko and H. Lemmetyinen, Electron-Transfer State of 9-Mesityl-10-methylacridinium Ion with a Much Longer Lifetime and Higher Energy Than That of the Natural Photosynthetic Reaction Center, *J. Am. Chem. Soc.*, 2004, **126**(6), 1600–1601, DOI: 10.1021/ja038656q.

34 P. T. Anastas and J. C. Warner, *Green Chemistry: Theory and Practice*, Oxford University Press, 2000.

35 F. A. Etzkorn, *Green Chemistry: Principles and Case Studies*, Royal Society of Chemistry, 2020.

36 H. Yan, J. Song, S. Zhu and H.-C. Xu, Synthesis of Acridinium Photocatalysts via Site-Selective C–H Alkylation, *CCS Chem.*, 2021, **3**(12), 317–325, DOI: 10.31635/ccschem.021.202000743.

37 A. R. White, L. Wang and D. A. Nicewicz, Synthesis and Characterization of Acridinium Dyes for Photoredox Catalysis, *Synlett*, 2019, **30**(7), 827–832, DOI: 10.1055/s-0037-1611744.

38 V. Srivastava, P. K. Singh, A. Srivastava and P. P. Singh, Synthetic applications of flavin photocatalysis: a review, *RSC Adv.*, 2021, **11**(23), 14251–14259, DOI: 10.1039/D1RA00925G.

39 J. Brandrup, E. H. Immergut and E. A. Grulke, *Polymer Handbook*, John Wiley & Sons, 1999.

40 D. W. V. Krevelen, *Properties of polymers: their correlation with chemical structure, their numerical estimation and prediction from additive group contributions*, Elsevier, 1990.

41 N. P. Ramirez, B. König and J. C. Gonzalez-Gomez, Decarboxylative Cyanation of Aliphatic Carboxylic Acids via Visible-Light Flavin Photocatalysis, *Org. Lett.*, 2019, **21**(5), 1368–1373, DOI: 10.1021/acs.orglett.9b00064.

42 The yields of isolated copolymer are 60–75%. The loss of material likely occurs due to material transfers during purification via dialysis and lyophilization. Please see Supporting Information for procedures.